75-2553

A System for the digital transmission of X-ray pictures over voice grade dial up channels using data compression and subsequent computer processing

Final Progress Report of the Research Contract under the title of A SYSTEM FOR THE DIGITAL TRANSMISSION OF X-RAY PICTURES OVER VOICE GRADE DIAL UP CHANNELS USING DATA COMPRESSION AND SUBSEQUENT COMPUTER PROCESSING by Dr. Kunio Takaya, Division of Biomedical Engineering University of Saskatchewan. Contract Serial Number: OSU5-0229.

1. INTRODUCTION

This report presents a summary of the work conducted during the period of November 1, 1975 to March 31, 1976 by the Division of Biomedical Engineering, University of Saskatchewan, Saskatoon, into the digital transmission of X-ray pictures over voice grade dial-up channels.

An image sensing device for the X-ray picture transmission has been developed by the preceding research study contract made under the same title. This image sensing device is in principle a mechanical laser scanner which utilizes He-Ne laser as a light source and two galvanometer beam deflectors to scan the laser beam over an X-ray film. The light passing through the X-ray transparency is then diffused by a diffuser and detected by a photomultiplier.

The major problem of the second phase of this research contract is the data compression on the large amount of pictorial information read from the X-ray film scanner. The implementation of a straightforward estimator, which estimates the incoming signal from the previous samples in the same scan line or the previous few lines, and an information entropy preserving code is discussed in this report.

In order to investigate the above mentioned major objective, it is essential to interface the X-ray film scanner to a computer. During the

period from November 1, 1975 to January 31, 1976, our efforts and time have been devoted to the development of a stand alone controller and a computer interface for this X-ray film scanner. Also, a slight modification to the already developed device has been made. A light tight cover was made for this X-ray film scanner to make it possible to operate under the normal room light. At the same time, the physical dimension was slightly reduced.

2. THE CONTROLLER AND COMPUTER INTERFACE FOR X-RAY FILM SCANNER

Although the controller and the computer interface should preferably provide versatile capabilities on its scanning mode, the following features were selected to attain fast data acquisition of a large amount of video signal and to avoid unnecessary complexity of the instrument. A controller for the X-ray film scanner has been developed with the capabilities:

1) Scanning over a whole X-ray film by continuous mode.
2) Localized scanning by continuous mode.
3) Multiple scanning or advanced scanning by single sweep mode.

A block diagram of the X-ray film scanner is shown in Fig. 1. The developed controller is independent of the computer to be connected. However, it requires the host computer to have a one channel Analog to Digital converter, 16 bit output buffer, and an external interrupt. The SDS Sigma II computer is currently used for the experiments of the second phase of this subject.

The horizontal axix (x-axis) is scanned by a triangular sweep signal generated by a low frequency function generator. The vertical axis (y-axis) is positioned by a digital to analog converter and a binary counter. Therefore, the control along x-axis such as centering beam, setting the scan width and the scanning speed must be manually preset. Whereas, the dual control feature was provided for the y-axis, so that the upper limit and the lower limit of the area to be scanned and the mode, either continuous or single sweep, can be set either by the computer or from the front panel of the X-ray film scanner. This is a convenience to view the scanning area before data acquisition.

The data acquisition procedure by the computer is as follows. MODE must be set if the continuous scanning mode is prefered. Upon providing the upper scanning limit on the digital buffer, LOAD must be activated to set the initial value on the binary counter. Then, the output buffer must maintain the lower limit until the scanning over the whole area of interest is completed. As soon as START is sent from the computer, the laser beam is driven by the triangular wave. When the position signal from the capacitive position sensor of the galvanometer beam deflector reaches a threshold corresponding to the leftmost position, a pulse is sent on the INTERRUPT line. This INTERRUPT starts the analog to digital conversion of the video signal. At the completion of one scan line, the binary counter is incremented to advance the y-position. If MODE is single mode and scanning other than successive scanning is desired, the beam position along y-axis must be set for every single scan.

The video signal from the photomultiplier is preamplified and then fed to a logarithmic amplifier to compress the large amplitude due to the excessive light at the transparent region of a film and to enhance the small signal at the darker region.

3. IMAGE DATA COLLECTION

The video signal from a photomultiplier is preamplified and then fed to a logarithmic amplifier to compress the large amplitude due to the excessive light at the transparent region of a film and to enhance the small signal at the darker region. The logarithmic amplifier being used in this system covers 4 decades of the input voltage from 10^{-3} volts to 10^{1} volts by ±4 volts of output. This compensates the exponential nonlinearity between the X-ray intensity and the silver grain concentration on an X-ray film. The DC level of the video signal from the photomultiplier is adjusted so that approximately 5% of the total deviation of the video signal produces a half of the total output change. The characteristics of the logarithmic amplifier is shown in Fig. 3. The input voltage at which the output voltage crosses zero is equivalent to 0.1 volts. The darker area is sensed, the more negative the output voltage becomes. Another amplifier after the logarithmic amplifier was provided to match the signal to the full scale of the AID converter, which is ±10 volts equivalent to 12 bits.

The video signal was digitized by SDS Sigma II computer and the sampled data were stored in a magnetic tape. The interruption signal was used to dump the accumulated data of a scan line in one of two buffers to the magnetic tape and to initiate the other buffer for storing incoming data. The developed laser scanner is capable of scanning 4 line/mm at its maximum resolution, the number of data cells in a scan line is 1400 and the horizontal scan lines are 1700 lines. However, a coarser sampling was used to create test data sets to investigate fundamental statistical characteristics of a chest X-ray picture and an abdominal X-ray pictures shown respectively in Fig. 4 and in Fig. 5. One thousand picture cells were sampled from a horizontal scan line whose length is approximately 12 inches. A test data set in a magnetic tape contains 1000 scan lines which covers vertical 15 inches. The time required to quantitize a whole picture was 400 seconds when sampling frequency 5 KHz was chosen, since the data were taken only during one direction of scan motion of the beam. The pictures reproduced on the oscilloscope for monitoring purpose are shown in Fig. 6.

4. COMPRESSION OF IMAGE DATA AND CODING

If a reduction in size is required for a large digitized data set of an X-ray picture and the use of the compressed data is to reproduce its image in a visible form, one may choose a less redundant code to represent the data and preserve whatever the information contained in the original data set. However, depending on the method employed in the image reproduction system, the difference between the originally digitized data and the compressed data could be tolerated to some extent in order to obtain the same visual impression. In this case, the information entropy is not necessarily preserved. The nonuniform quantitizer and the transfrom coding using orthogonal functions such as Hadamard transform are classified in this category. Since the image reproduction device necessary at a receiving end has not been developed yet, the discussion in this report is limited in entropy preserving data compression.

The image data measured in terms of light intensity are usually highly correlated to its neighborhood. If the proximity data of a particular image cell of interest are given, the value of the cell can be estimated with a high accuracy. Therefore, successful data compression largely depends on the estimation method to be used. The most common way of the image coding is to utilize the estimation error from the true outcome as the input to the coder, which generates less redundant codes. There are actually two mechanisms involved in data compression. One is proper choice of the estimator and the other is the efficient code. Different estimators and code systems were experimentally assessed for two test data sets, a chest X-ray picture and an abdominal X-ray picture.

A. Estimators

The autocorrelation curves of two scan lines are shown in Fig. 7, the ordinate of which is the distance shifted for integration and its full scale is equivalent to 1000 picture cell distance. The width of the center peak of these auto-correlations is approximately 50, so that any picture cell within the radius of 25 picture cell distance from the center cell is highly correlated to each other. A question arising from the auto-correlation is how far data should be taken into consideration to estimate a new data. Since the test data set is a raster scanned data, only available data for estimation are only those scanned previously, either in the same scan line or in the previous lines.

Three kinds of simple estimators have been tested and and evaluated in terms of the information entropy of the estimation error. The simplest is to use the value of only one previous sample as best estimate $\overline{X}i$.

1. $\overline{X}_{ij} = X_{i-1,j}$

The second method uses already sampled adjacent cells, i.e. three consequentive data in previous scan line located above the cell to be estimated plus a previous datum in the current scan line.

2. $\overline{X}_{i,j} = 1/4(X_{i-1,j-1} + X_{i,j-1} + X_{i+1,j-1} + X_{i-1,j})$

The third method addstwo more cells to the second method located horizontally or vertically at two cell distance away from the cell to be estimated. Therefore, the third method requires two previous lines.

3. $\overline{X}_{i,j} = 1/6(X_{i,j-2} + X_{i-1,j-1} + X_{i,j-1} + X_{i+1,j-1} + X_{i-2,j} + X_{i-1,j})$

In order to compare those estimators, the information entropies of the estimation error, which is simply the difference between the true outcome and the stimated value, were computed. If the estimation error concentrates around zero, the information entropy

$$H = -\sum_{i=-1024}^{i=+1024} \rho_i \log \quad \rho_i \log_2 \rho i$$

would be less than that of the wide spread error occurence. Where, Pi is the probability for an error value i to occur. A portion of a picture consisting of 50 scan lines were arbitrarily chosen from each test data set and the histograms of the original data and the different estimation errors were computed. Then, the mean values, the standard deviations and the information entropies were calculated from the probability density functions obtained from the histograms. The results of computations were shown in the following table.

	Mean	S.D.	Entropy
Chest X-ray Picture	-157.50	190.25	8.33
Estimator 1	0.02	21.69	6.27
Estimator 2	-0.34	34.99	6.86
Estimator 3	-0.39	32.29	6.78
Abdominal X-ray Picture	66.38	166.76	8.81
Estimator 1	-0.05	13.41	5.61
Estimator 2	40.82	18.02	5.83
Estimator 3	0.88	16.34	5.73

Table 1

This results indicates that the original data sets whose information length is 11 bits have 8~9 bits of average information per picture cell without considering the correlation of a cell to another. In another word, the redundancy of the original data sets is 2~3 bits if it is assumed that the image is an uncorrelated image. Since the actual image is not uncorrelated, further reduction of the information entropy is possible by introducing an estimator in conjunction with a differentiator. Among three tested estimators, the estimator 1 most reduced the entropy. The information entropy of the estimation error of estimator 1 was 2~3 bits less than that of the original data sets. Other two more complex estimator did not show so remarkable reduction as expected. This is partially because of the slightly wider raster interval than inter-cell distance in a scan line, which gives a poorer correlation. Another reason worth noting is a property of average estimators. When a larger area is used for averaging, the high frequency response of spatial transfer function usually deteriorates. Yet, the original data contains high frequency components and is not so smooth as the stimated signal. Unless weighting factors for the image cells being considered in estimation are properly chosen, the more priori data do not always improve the performance of the estimator. For instance, in order to realize an ideal high-cut filter, the weighting factors must be numerically chosen according to a sinc function, which is an inverse Fourier transfrom of a rectangular frequency response. This requires the estimator to cover a large readily sampled area. The estimators which use previous lines need a far larger memory space, 1K~2K bytes, compared to the only one data space required by the estimator 1. It seems, therefore, desirable to use the estimator 1 and form a well-known DPCM (Differential Pulse Coded Modulation) for the first step of compressing data.

The wave forms of digitized video signal of a chest X-ray picture and an abdominal X-ray picture were shown respectively in Fig. 8 and in Fig. 13. The histograms of the original data sets are shown in Fig. 9 and Fig. 14. The histograms of the estimation error shown in Fig. 10 and in Fig. 15 are computed by the estimation method 1. Fig. 11 and Fig. 16 are those based on estimation method 2. Fig. 12 and Fig. 17 are those based on the estimation method 3. The former figure of a kind is the chest X-ray picture and the latter is the abdominal X-ray picture.

B. Encoders

The standard deviations and the entropies shown in Table 1 indicate that the information entropies of DPCM are in the range of 5~6.5 bits/pic. cell and nearly 68% data (±S.D.) fall within 5 bits/pic. cell (±15) when the initially sampled 11 bit data are used. Since the above mentioned entropies are the attainable lower limit by an ideal code constructed under the assumption of an uncorrelated image, further reduction requires a coarser quantitzation level. Though it is not known yet how many distinguishable grey tone can be realized by a printer under consideration, the earlier workers have suggested that 6 bits on logarithmic grey scale are enough to give continuous visual impression, i.e. analog image. Therefore, a coarser quantitzation, 9 bits including sign, was used in what follows. This makes it possible to fit the differential signal into 5 bits with almost no exceptions. In order to construct effective code systems to compress the image data, the 5 bit difference signal is considered as input to encoder. The profile of a difference signal shown in Fig. 19 is obtained from a scan line signal in Fig. 18. The correlation between samples is obviously removed.

The aim of the code design is to make an efficient entropy preserving code, which is decodable into the exactly same information as input. In case of entropy preserving codes, the average word length per picture cell is bounded by the information entropy computed from a probability density function under consideration. The lower limit of the coder, which does not take the transition from a sample to another into account is given by the probability of occurence of each value of 5 bits. When a coder design is based on the 1st order Markov chain model, the information entropy computed from the conditional probability of transition gives the lower limit.

$$H = -\sum_{i=-16}^{16} \rho(i) \sum_{j=-16}^{16} \rho(j|i) \log_2 \rho(j|i)$$

The lower bounds of word length are computed for two coders with transition and without transition.

	Without transition	With transition
Chest X-ray picture	3.82 bits	3.64 bits
Abdominal X-ray picture	3.77 bits	3.69 bits

Table 2

As far as the lower bounds shown in the above table are concerned, there is not a significant difference between two coding schemes. This means that the correlation involved in two samples is well removed by taking the difference between a current sample and a previous sample. Therefore, it is not important to consider whether or not the transition in Markov's sense should be taken into consideration when a code system is designed. If the well-known Shannon-Fano method or the Huffman's method is used, the average word length of code will be very close to one of the above mentioned limits. However, there is another question to answer. Is the variable length code suitable for this particular transmission system? The binary code sequence generated by the Shannon-Fano method or the Huffman's method is uniquely decodable but is not instanteneously decodable. The end of any code word cannot be recognized without the need of inspection of succeeding code symbols. Any error occurred during actual transmission makes the associated decoder unable to find the proper boundary between code words or causes serious error propergation. It is practically done to place additional bits for error detection or error correction. To employ the available technique in regard to error detectable and error correctable codes, it is more convenient to use a fixed length code rather than variable length codes. When an efficient fixed length code system is desired, a possible way is to use the group code, in which a code represents a particular transition sequence. If a highly frequent sequence over a few samples is grouped and represented by the same code word length as an independent variable with a high frequency of occurence, it is possible to shorten the transmission time.

Two fixed length code systems were experimented. The frequency of occurrence is concentrated in the vicinity of zero. The highly frequent transitions are also limited within the vicinity of zero. Therefore, the coding method 1 considered only the transition among -1, 0, +1. A single step transition between two consequentive samples and two step transition over three successive samples were taken into account. In the second method, single transitions among -2, -1, 0, +1, +2 and the run-length of successive zeros up to 8 zeros are considered. The histograms of these two methods are shown in Fig. 20. The frequency of occurrence was computed from the test data of a chest X-ray picture. The peak existing around zero of the simple histogram has diminished and redistributed into group codes representing transitions.

	Chest X-ray Picture	Abdominal X-ray Picture
Method 1		
Single data	69472	74543
Single transition	6108	5507
Double transition	5761	4461
Total code sent (6 bits)	81341	84511
Total data sampled (5 bits)	98901	98901
Efficiency	0.987	1.025
Entropy	4.93	5.12
Method 2		
Single data	49550	53643
Single transition	22536	21261
Run-length 2 zeros	1385	1002
3	175	179
4	113	38
5	10	14
6	45	7
7	42	0
8	0	1
Total code sent (6 bits)	73856	76148
Total data sampled (5 bits)	98901	98901
Efficiency	0.896	0.924
Entropy	4.48	4.62

Table 3

The above Table 3 summarizes the performance of the experimented two code systems. When the group code of a fixed length is introduced to flatten the highly concentrated probability distribution, extra codes to represent the transitions must be provided in the expense of additional bits. In these two code systems, one additional bit was introduced. Therefore, unless those newly introduced transitions have relatively high frequency of occurrence compared with the ungrouped data, the total information size will not be drastically reduced. The Table 3 is self explanatory about the fact that the wider range rather than more steps of transition produces a better result. The method-2 which considers single transitions among ±2, ±1, 0 is better than the method 1. However, the reduction is approximately 10% and the code word length 4.5 is greater than the lower limits shown in Table-2.

5. CONCLUSION

Several techniques suitable to compress the enromous image data of an X-ray picture have been discussed. However, those experimented data compression methods were limited in the so-called entropy preserving methods. A coder designed under this category generates the codes which an appropriate decoder can recover the complete input information. Other compression techniques based on the printer characteristics and the visual sense are left for the future study of this project, since the printing device which reproduces an X-ray image on photographic transparencies has not yet developed and there are no means to assess the quality of the reproduced prints.

When the darkness information of an X-ray picture, which is proportional to the silver grain concentration on the X-ray transparency, is sensed by a light beam passing through the transparency and the exponentially saturated nonlinearity is compensated by the logarithmic compander, the final information is somewhat a linear function of the X-ray intensity transversed through a human subject. When the maximum deviation of this signal is digitized into 9 bits for example, the redundancy involved in the X-ray picture is approximately 3 bits without considering the correlation between samples, so that the real information is 6 bits. If the first order Markov chain model is introduced and the entropy is obtained from the conditional probabilities of transition, another 2 bits becomes redundant. Approximately 4 bits out of 9 bits are necessary code word length to describe the given image.

In order to reduce the data size to this theoretical bound, the best way found experimentally is to use a simple estimator whose output is simply the previously sampled adjacent datum and adopt a conventional DPCM system. By using the differential signal instead of the original video signal as input to a coder, 5 bits are sufficient to represent a picture cell and the redundancy of 4 bits is already removed. Since the probability function of the differential signal is Gaussian, any efficient code system such as Shannon-Fano's code and Huffman's code, which assigns shorter code words to more frequent values and longer code words to less frequent values, can reduce the data size at least 1 more bit. However, if the fixed length code is more adequate than the variable length code, highly frequent single step transitions within the vicinity of zero can be grouped and represented by a code word. This is, however, not so efficient because additional bits are required to cover the augmented transition groups. Only a 10% of reduction (0.5 bits) is achieved.

If a picture sampled at 1,400 picture cells per scan line and 1,700 scan lines per a picture it to be sent over 2,400 bps telephone channels, it takes 16.52 minutes even though the information per picture cell is only 1 bit. This indicates that such an image transmission system can never be realized solely by a entropy preserving coding method.

Other methods such as non-uniform quantizer, coarse quantitzation with dither pattern insertion and elimination of less significant image frequency seem to be promising. These methods reduce the information entropy as well as the data size. As long as there is not an image reproduction device available, these methods are left for future study.

To obtain some indication of the quality of the reproduced picture at the receiving end, investigations has been carried out into converting the present X-ray film scanner unit to a laser printer capable of reproducing a complete high resolution X-ray picture. The block diagram shown in Fig. 21 is a scheme being considered to modify the X-ray film scanner. The processed image data is fed into a signal processor to produce the modulation signal. This modulation signal is an input signal to an Acoustic Optical Modulator (Zenith M-40R Light Modulator), which modulates the intensity of the laser beam. The He-Ne laser beam is deflected in exactly same manner as the image data was collected. The modulated laser beam exposes a positive film which is sensitive to the read light. By this slight modification to the existing X-ray film scanner, a means of reproducing the X-ray picture will be provided.

REFERENCES

1. Lippel, B. and Karland, M.: "The Effect of Dither on Luminance Quantization of Pictures, IEEE trans." Com-19, 6, 879, 1971.

2. Chow, M.: "Variable-Length Redundancy Removal Coders Differentially Coded Video Telephone Signals, IEEE Trans." Com-19, 6, 923, 1971.

3. Rice, R.F. and Plaunt, J.R.: "Adaptive Variable-Length Coding for Efficient Compression of Spacecraft Television Data, IEEE Trans." Com-19, 6, 889, 1971.

4. Bell Telephone Lab: "Transmission Systems for Communication", Bell Telephone Lab, 1970.

5. Ingels, F.S.: "Information and Coding Theory", Intext Educational Publisher, 1971.

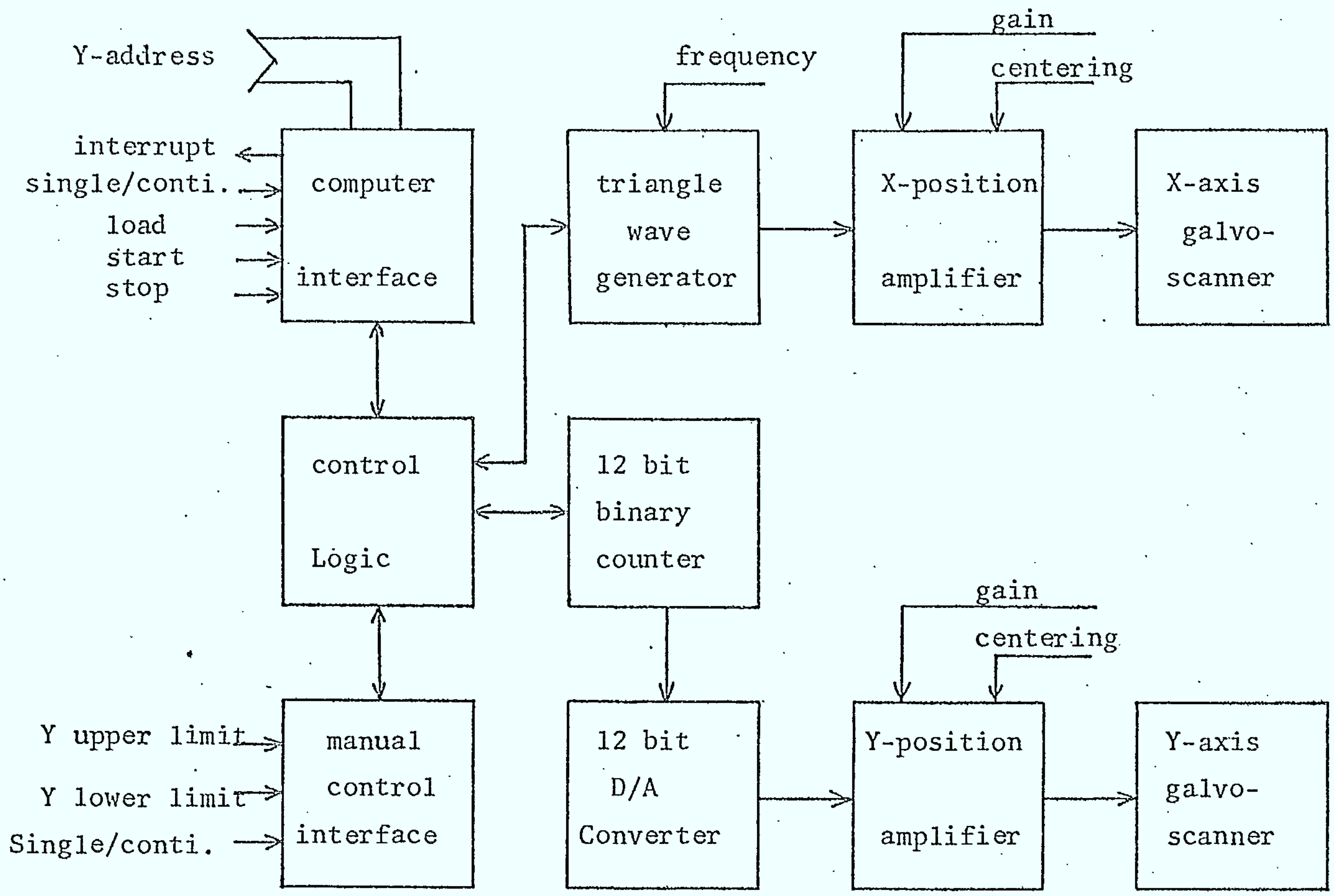

Fig. 1. The block diagram of the control interface made for the X-ray film scanner.

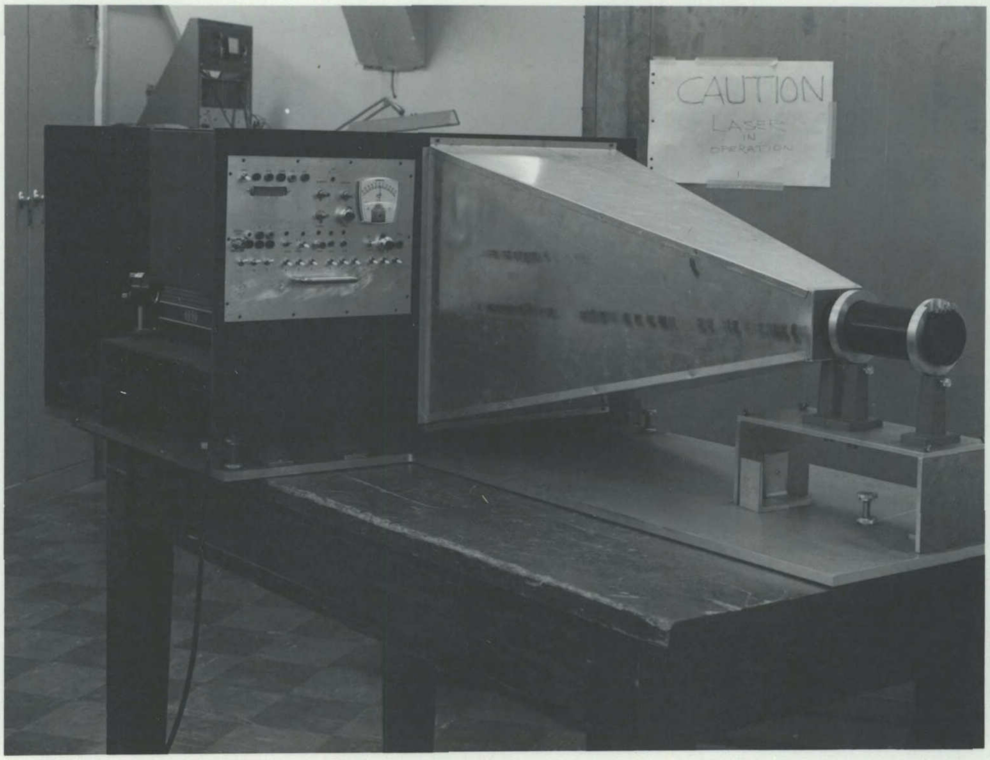

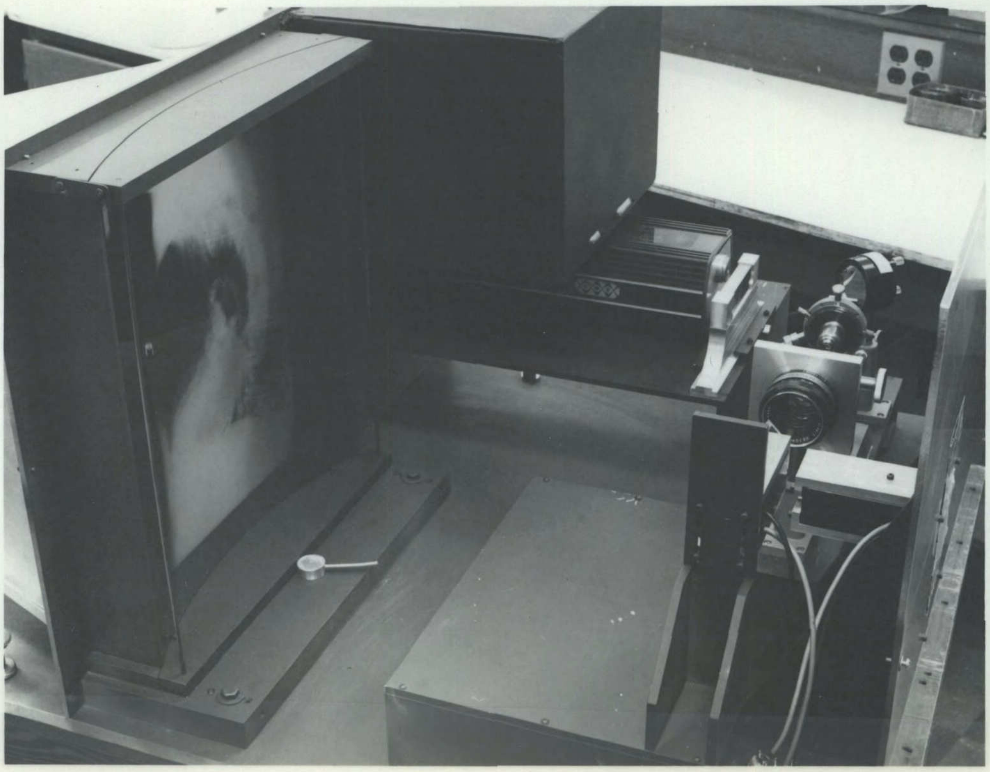

Fig. 2 A side view of the developed laser scanner (upper) and its inside (bottom).

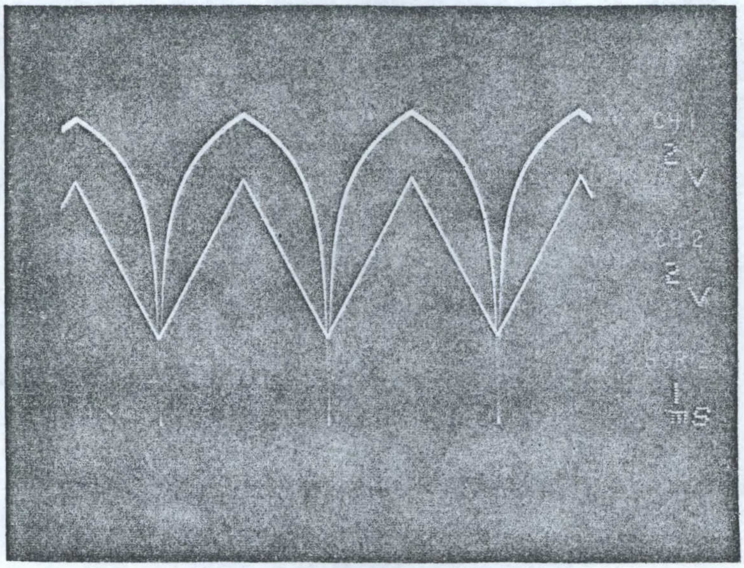

Fig. 3 The characteristic curve of the logarithmic amplifier in use.

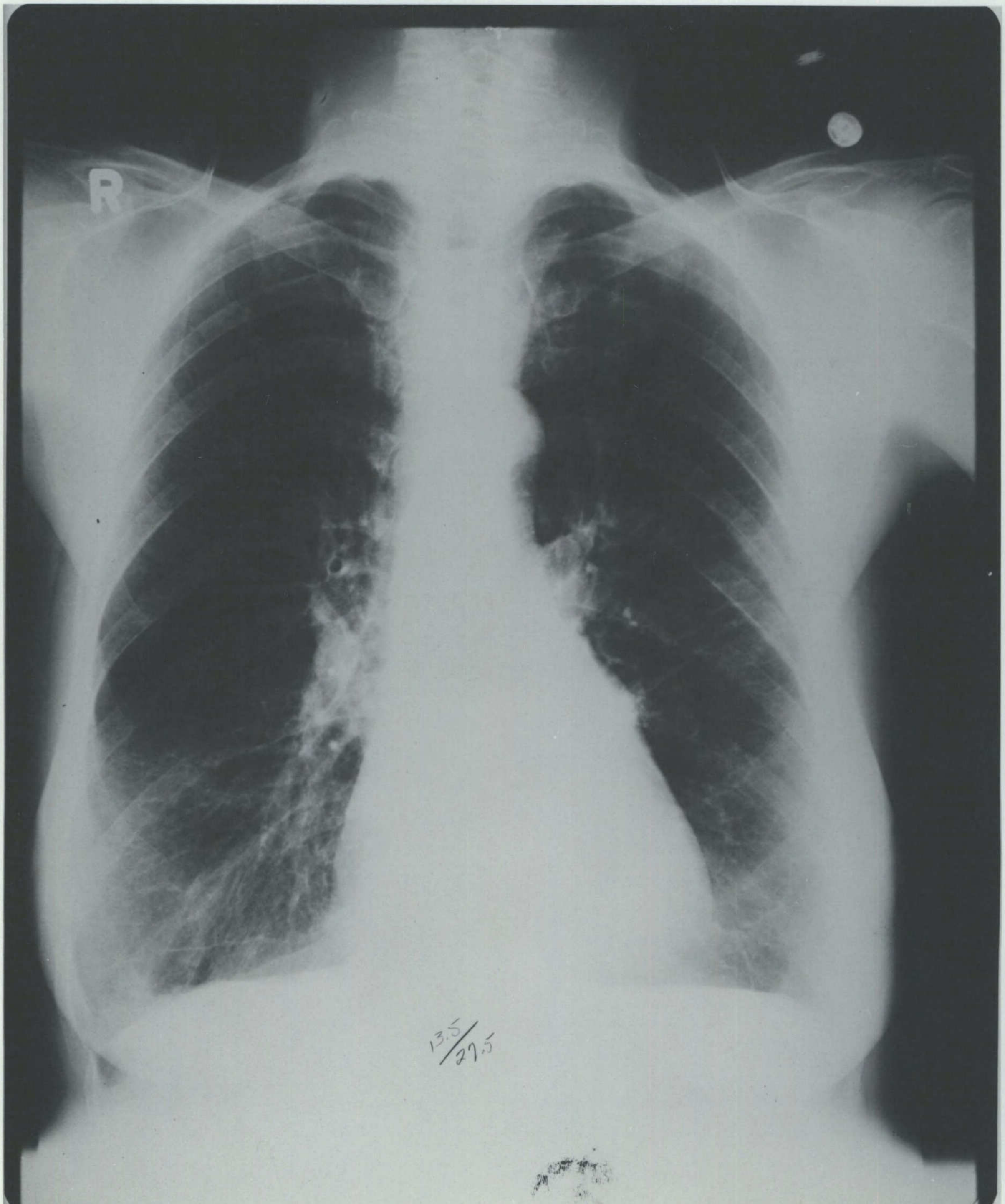

Fig. 4 A chest X-ray picture used for experiments.

Fig 4. A chest-x-ray picture used for test

Fig. 5 An abdominal X-ray picture used for experiments.

Fig 5. An abdominal - x-ray picture used for test

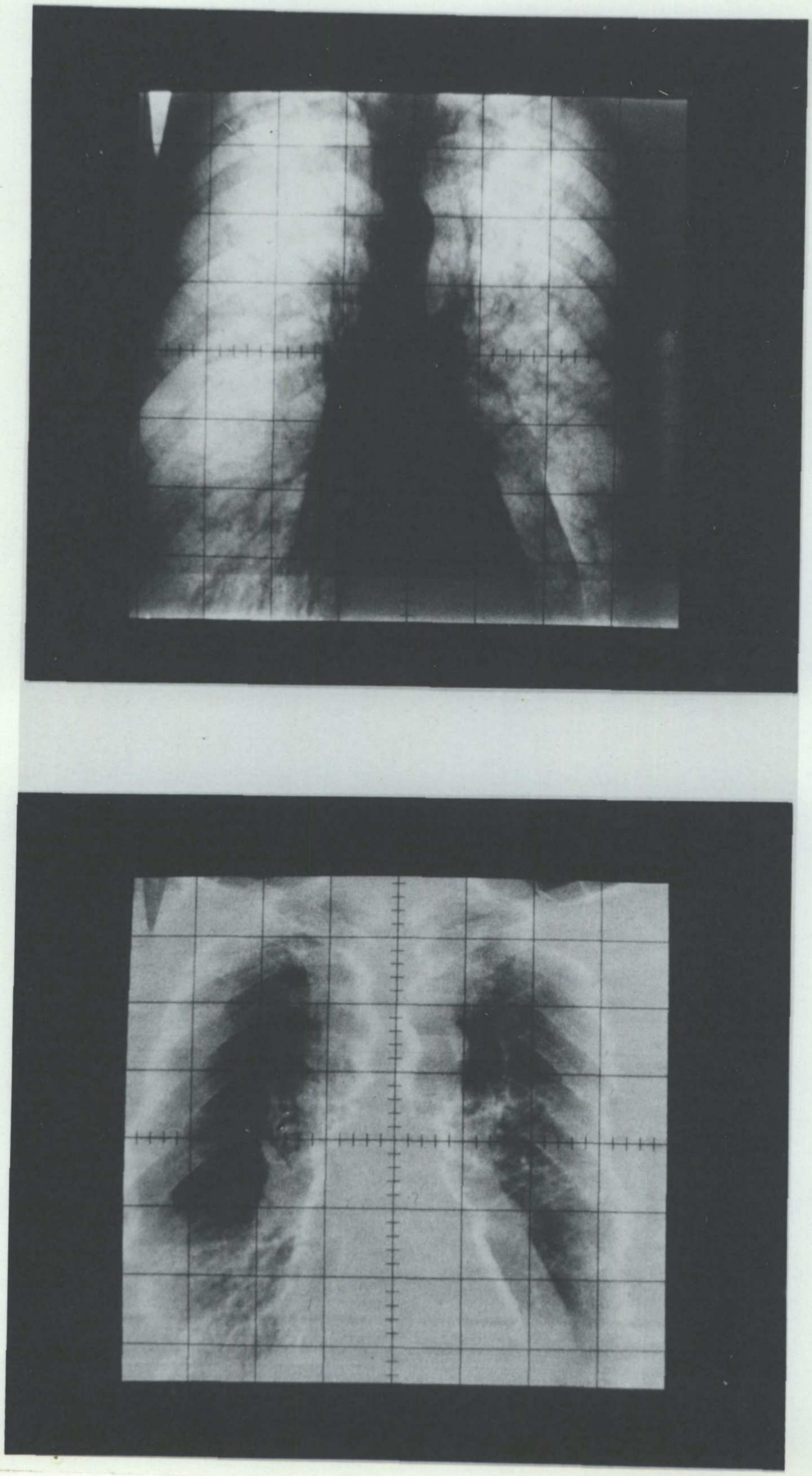

Fig. 6 Reproduced X-ray images on an oscilloscope for monitoring. The upper is black/white inverted. The lower is non inverted.

Fig 6 Reproduced pictures on oscilloscope for monitoring
upper inverted
lower non-inverted

Fig. 7 Auto-correlation curves (left) of arbitrarily selected scan lines (right). The upper frames are of a chest X-ray picture. The lower frames are of an abdominal X-ray picture.

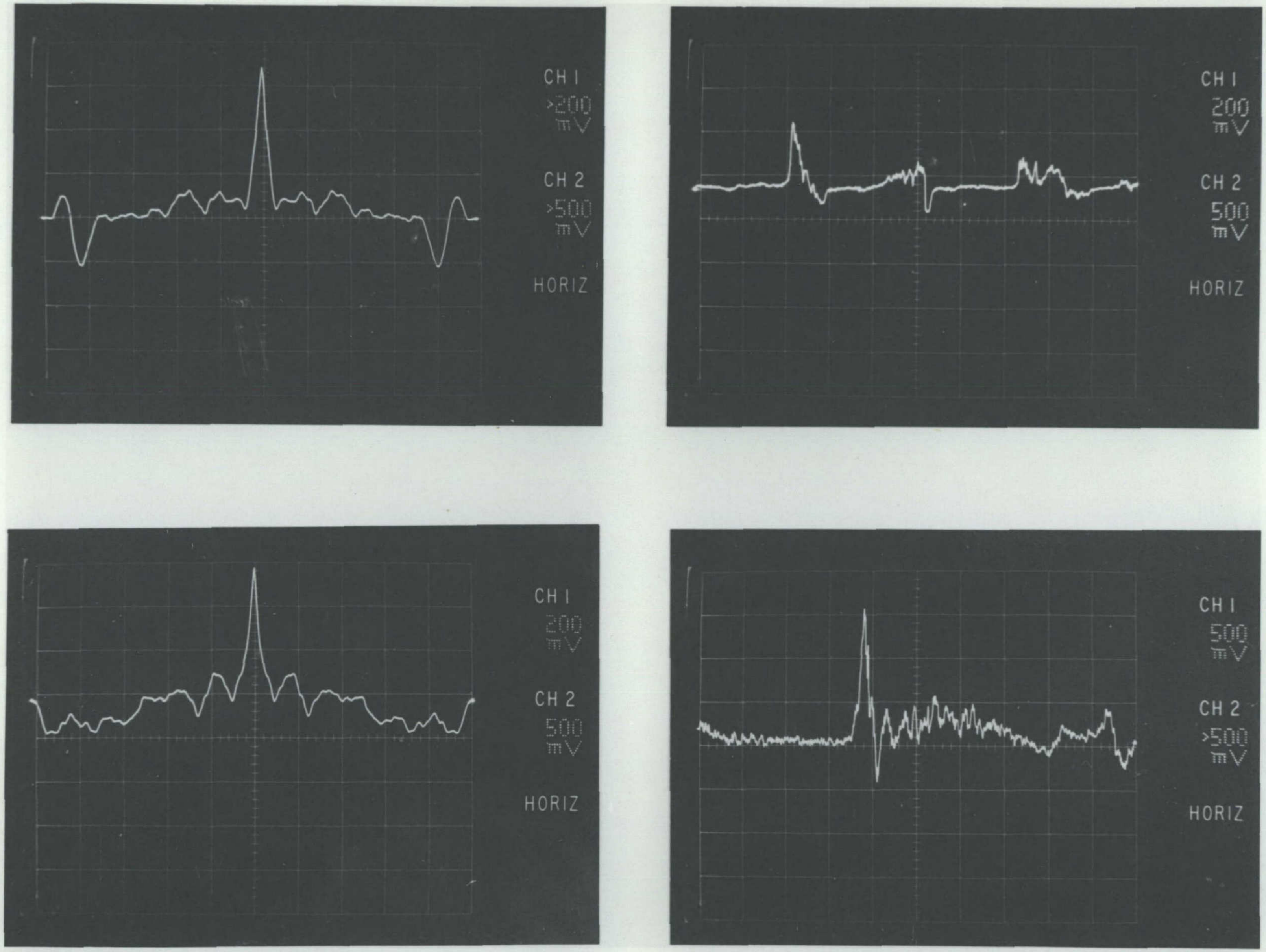

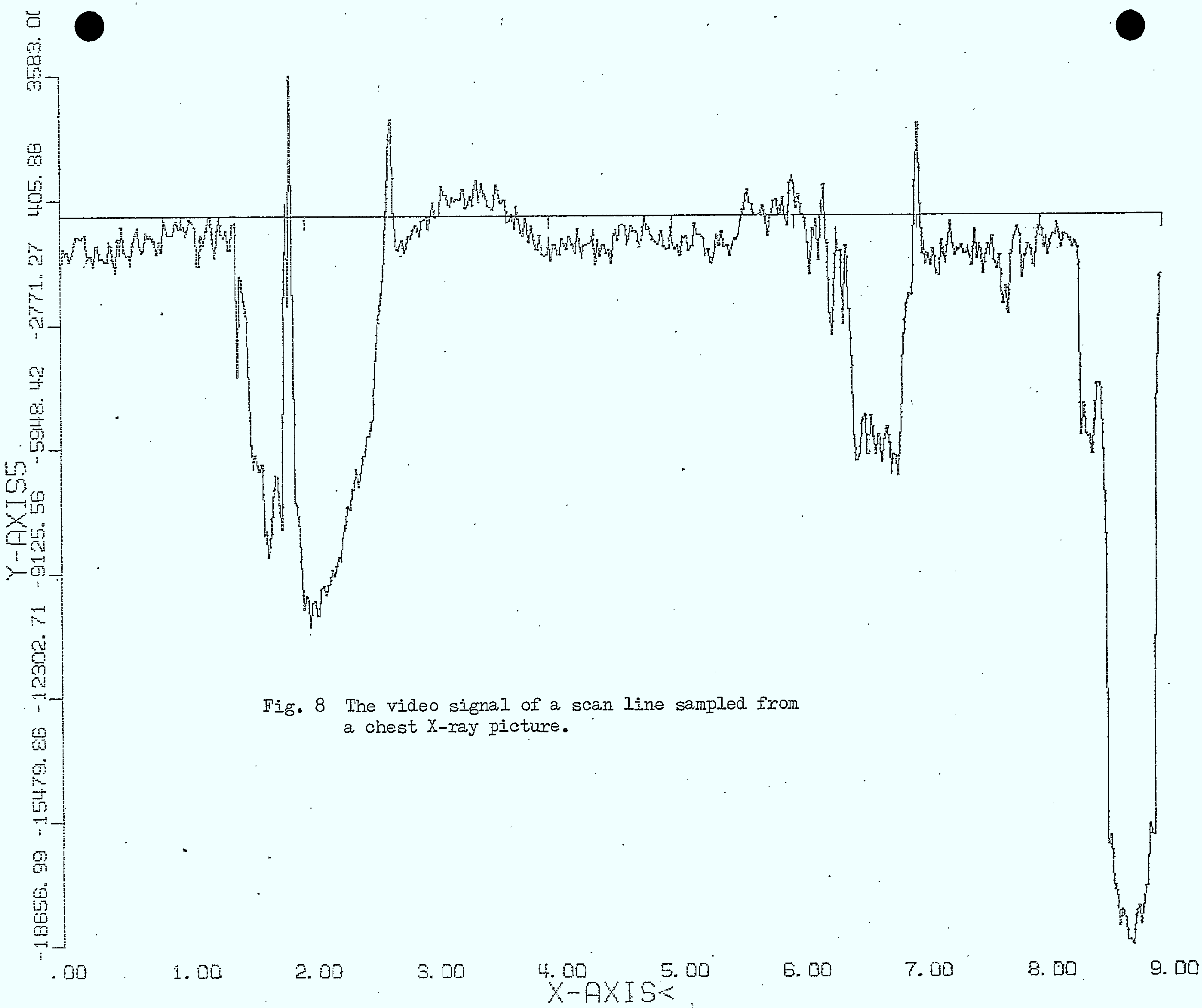

Fig. 8 The video signal of a scan line sampled from a chest X-ray picture.

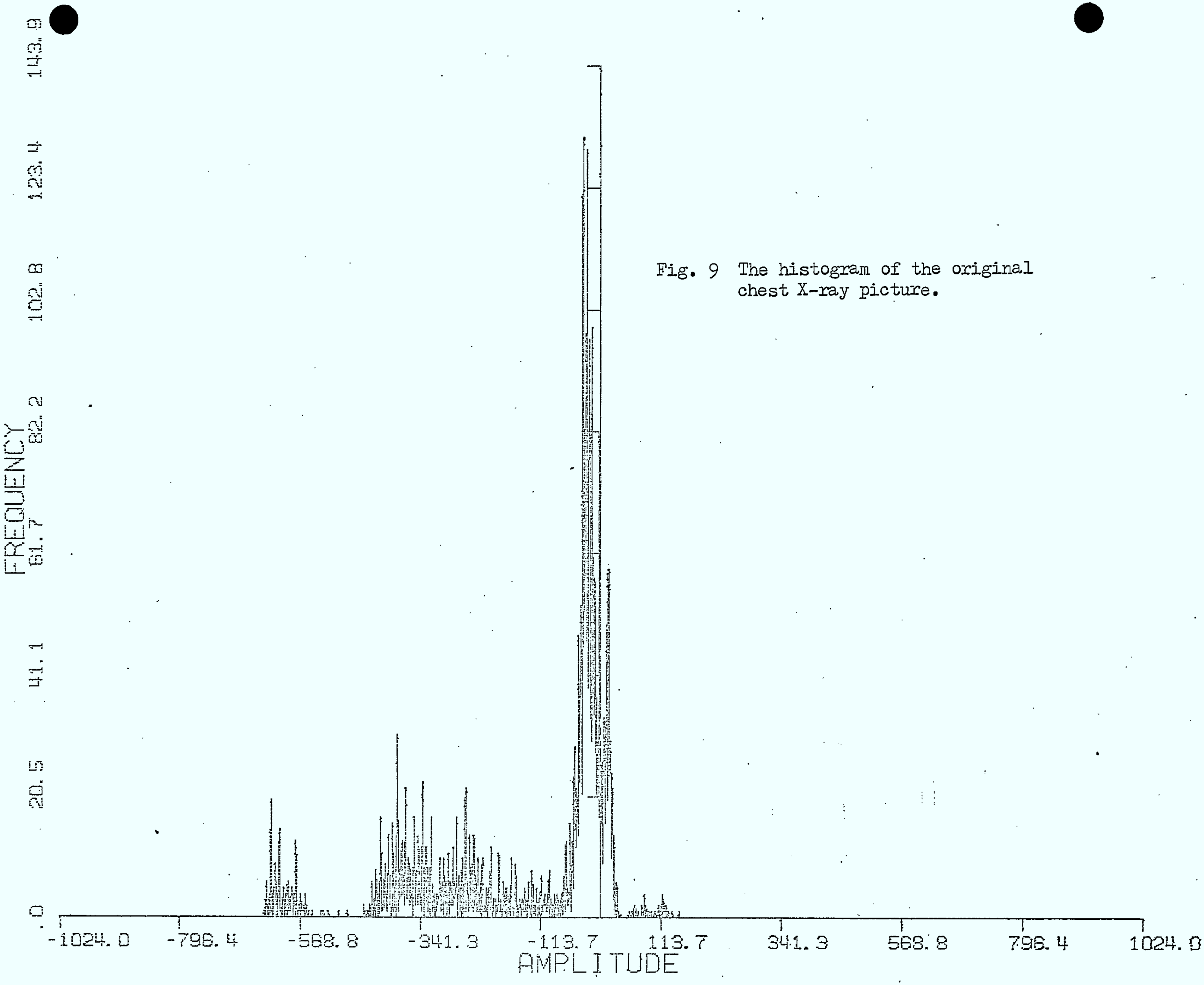

Fig. 9 The histogram of the original chest X-ray picture.

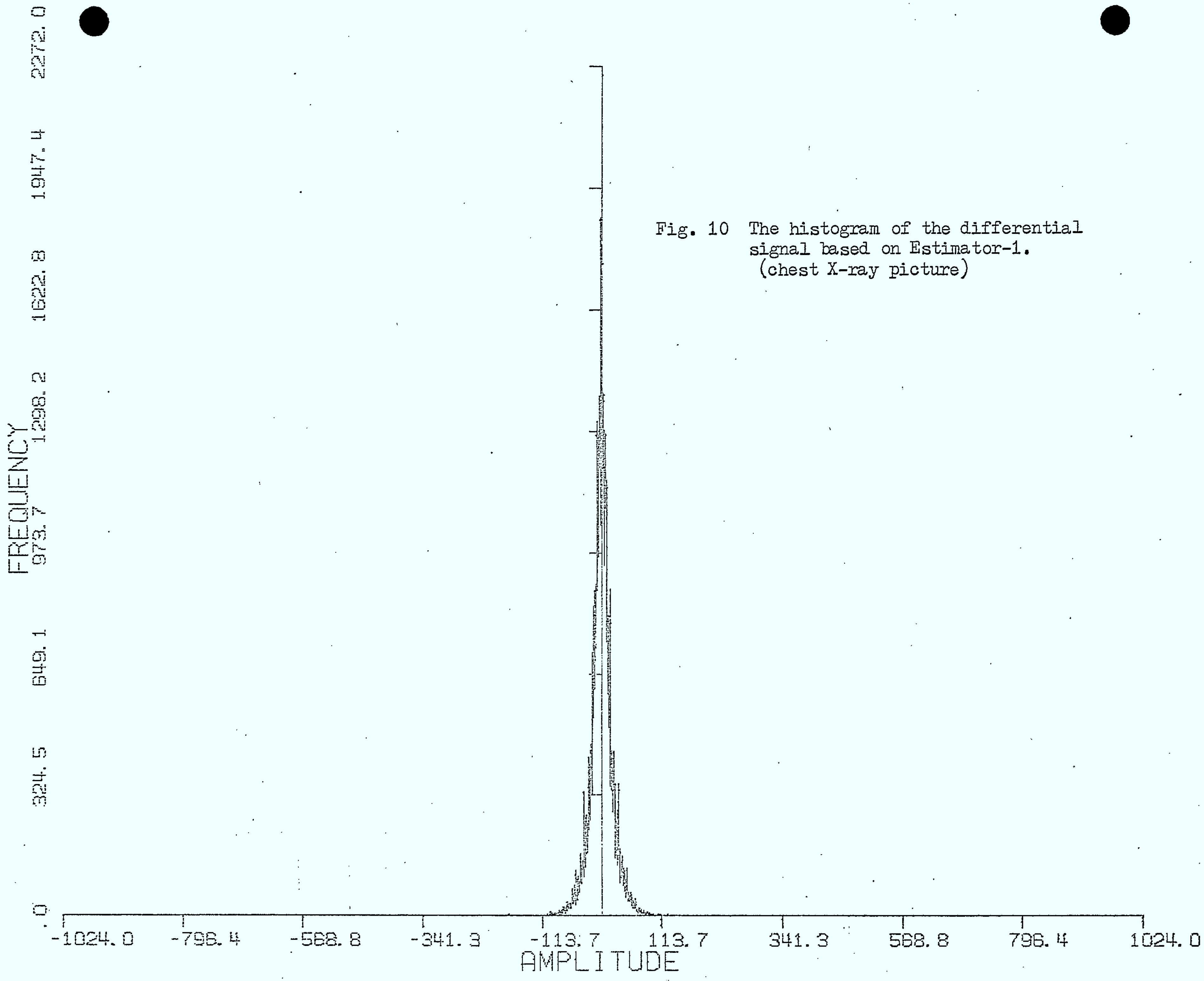

Fig. 10 The histogram of the differential signal based on Estimator-1. (chest X-ray picture)

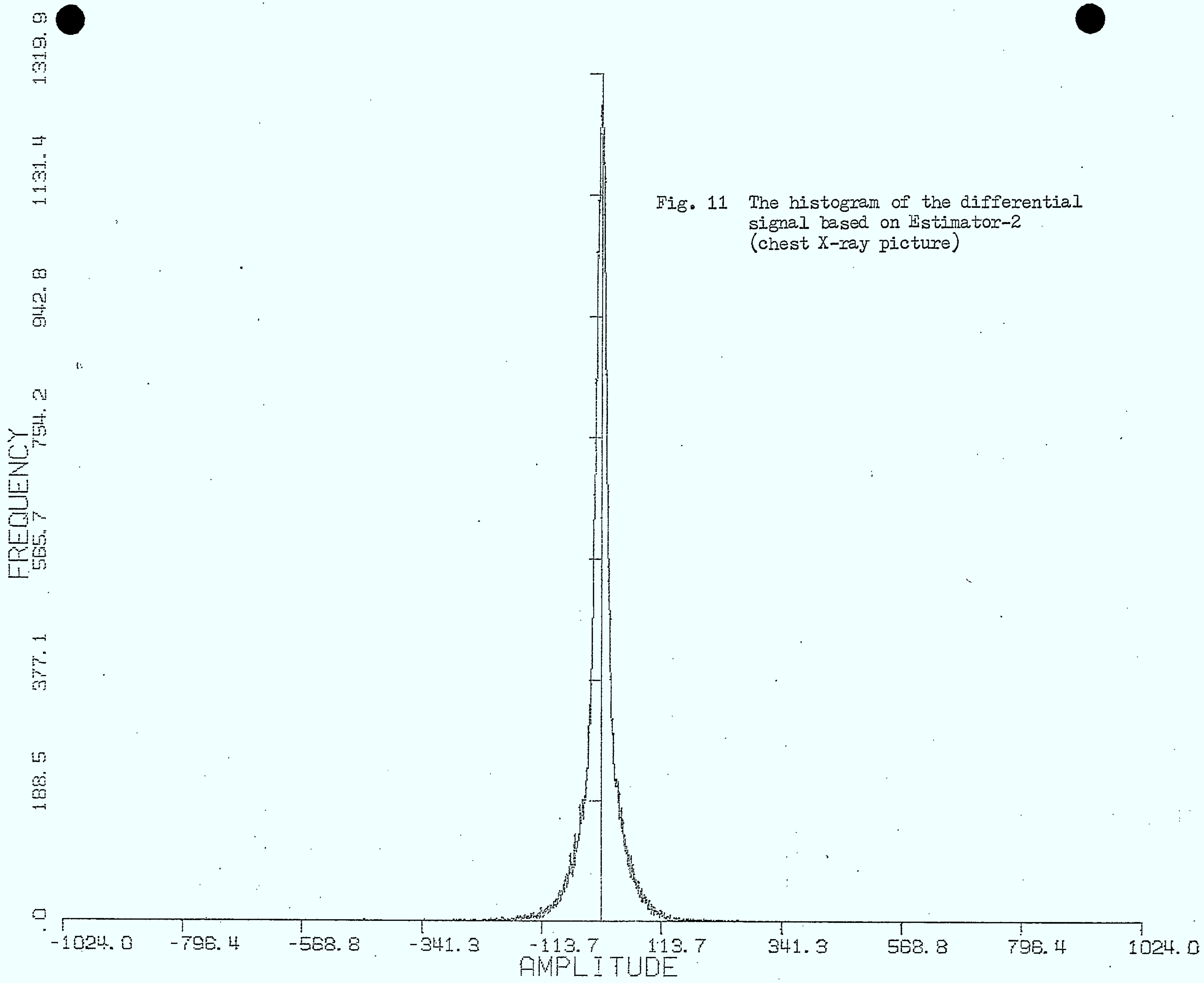

Fig. 11 The histogram of the differential signal based on Estimator-2 (chest X-ray picture)

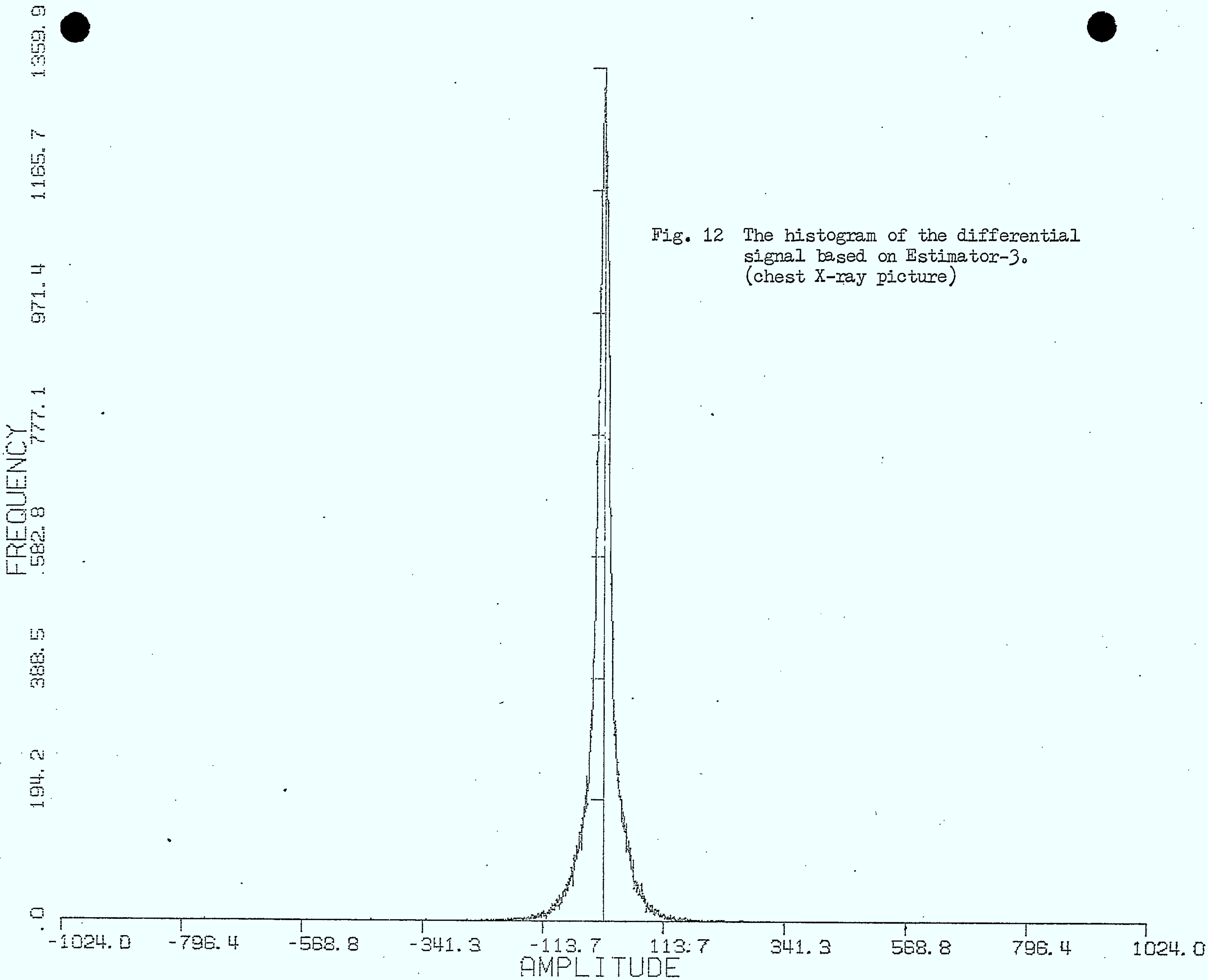

Fig. 12 The histogram of the differential signal based on Estimator-3. (chest X-ray picture)

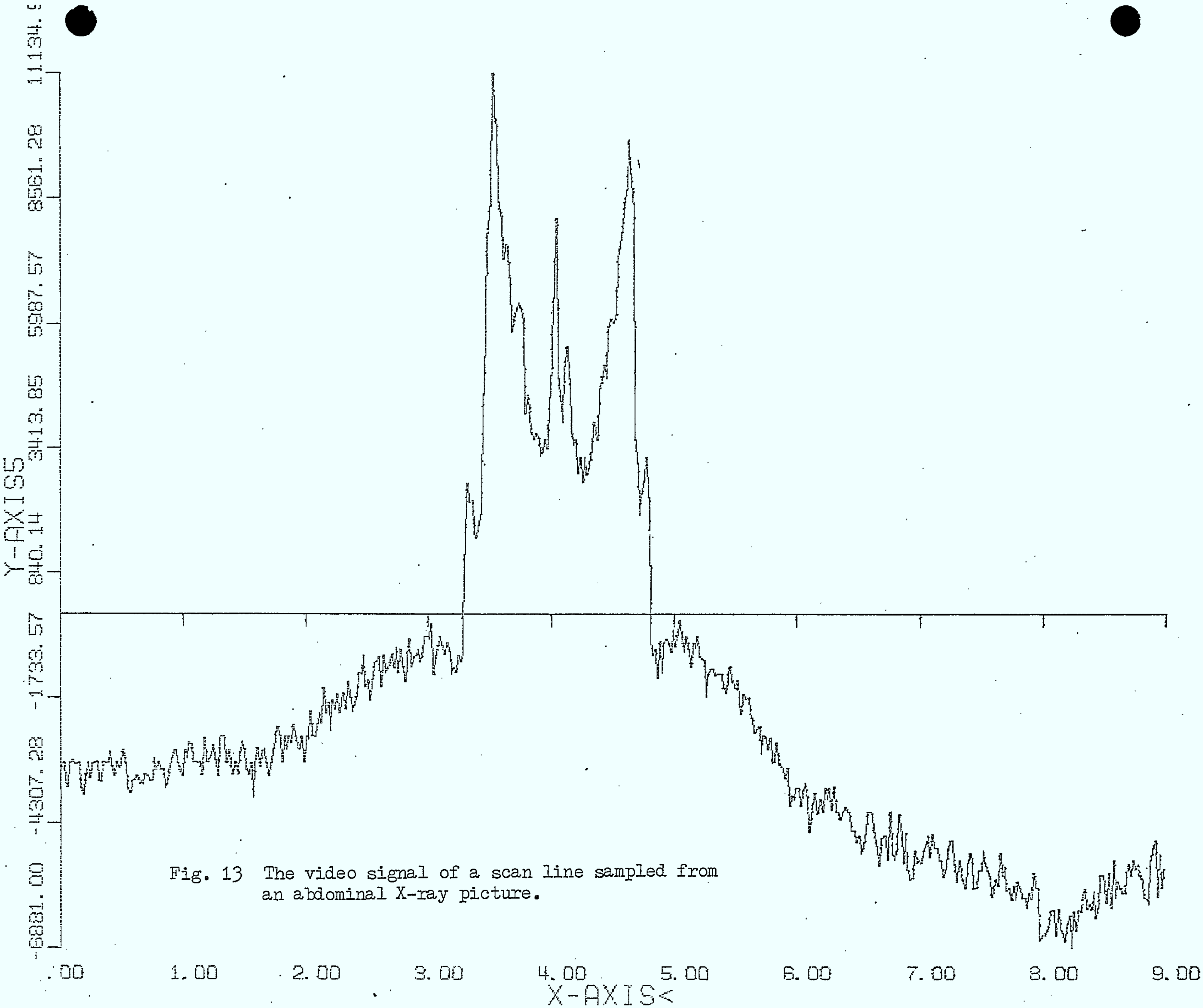

Fig. 13 The video signal of a scan line sampled from an abdominal X-ray picture.

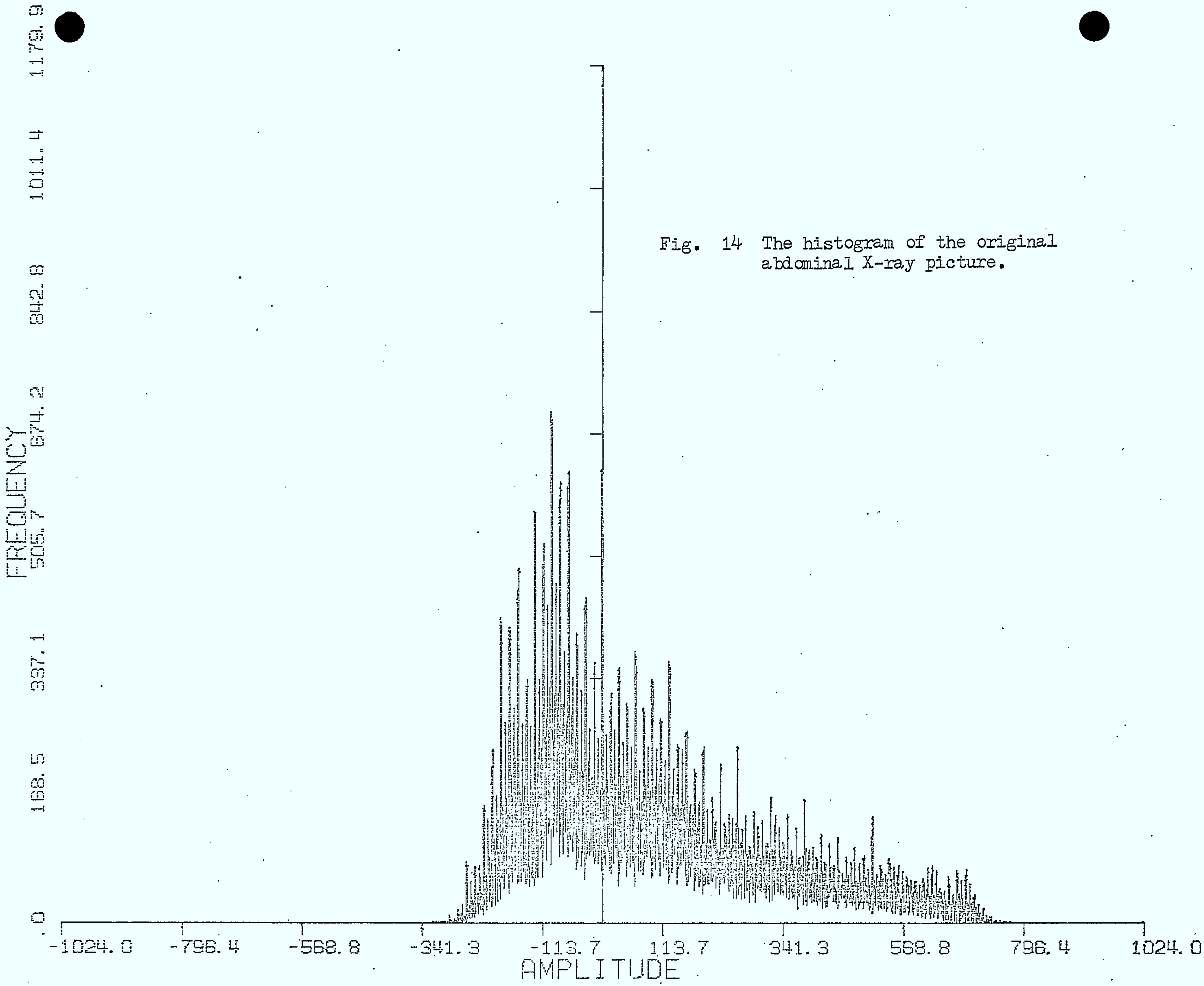

Fig. 14 The histogram of the original abdominal X-ray picture.

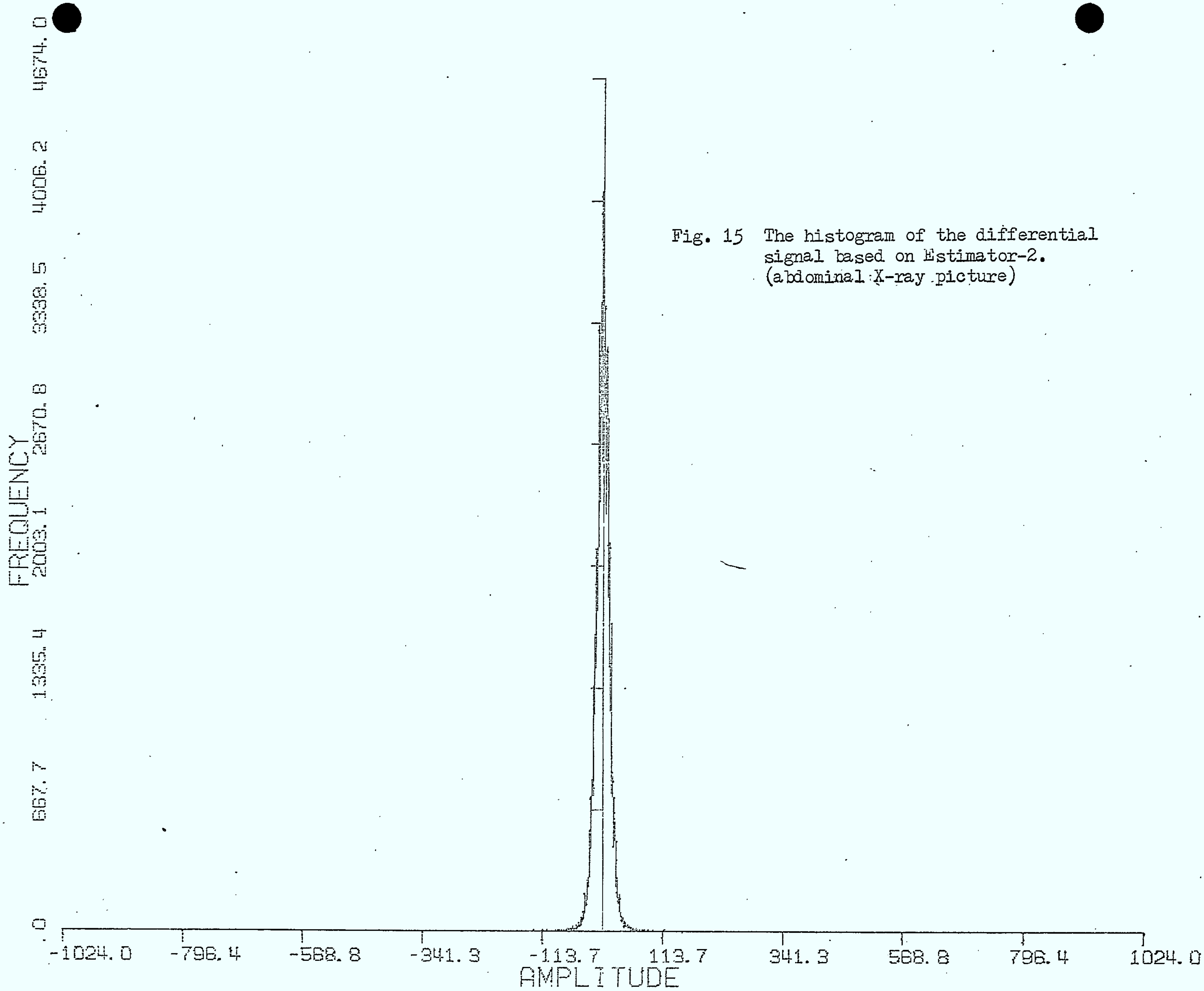

Fig. 15 The histogram of the differential signal based on Estimator-2. (abdominal X-ray picture)

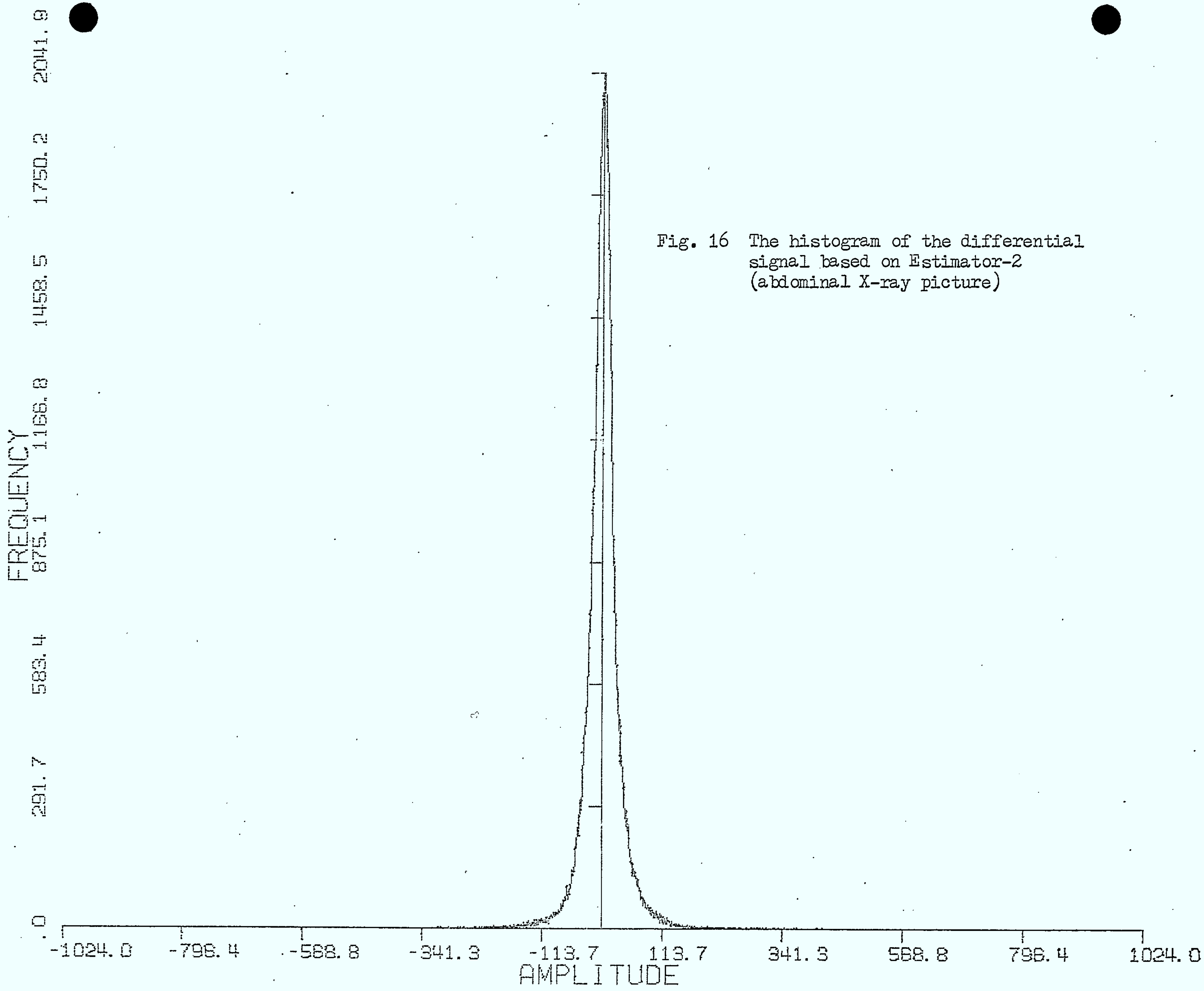

Fig. 16 The histogram of the differential signal based on Estimator-2 (abdominal X-ray picture)

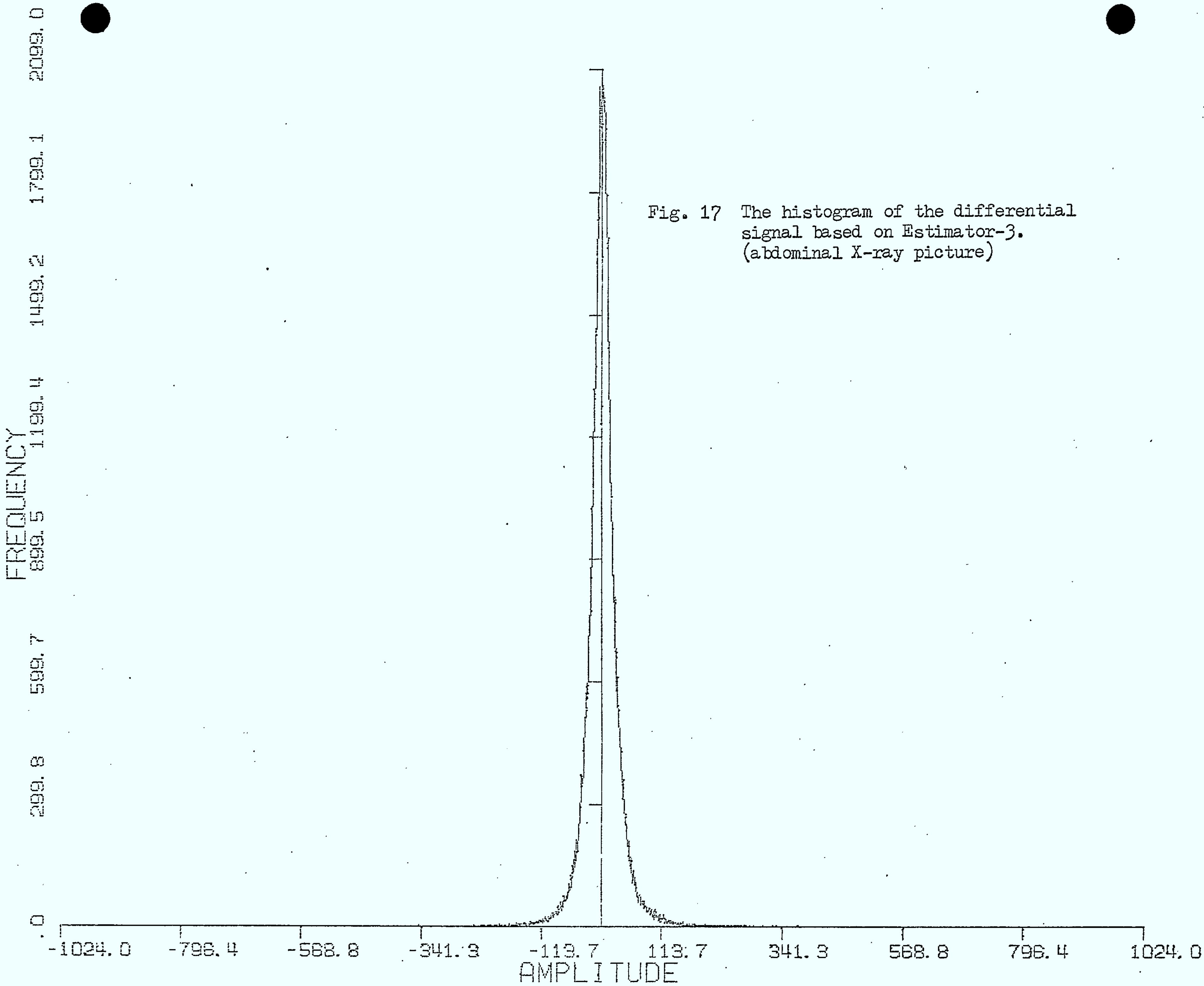

Fig. 17 The histogram of the differential signal based on Estimator-3. (abdominal X-ray picture)

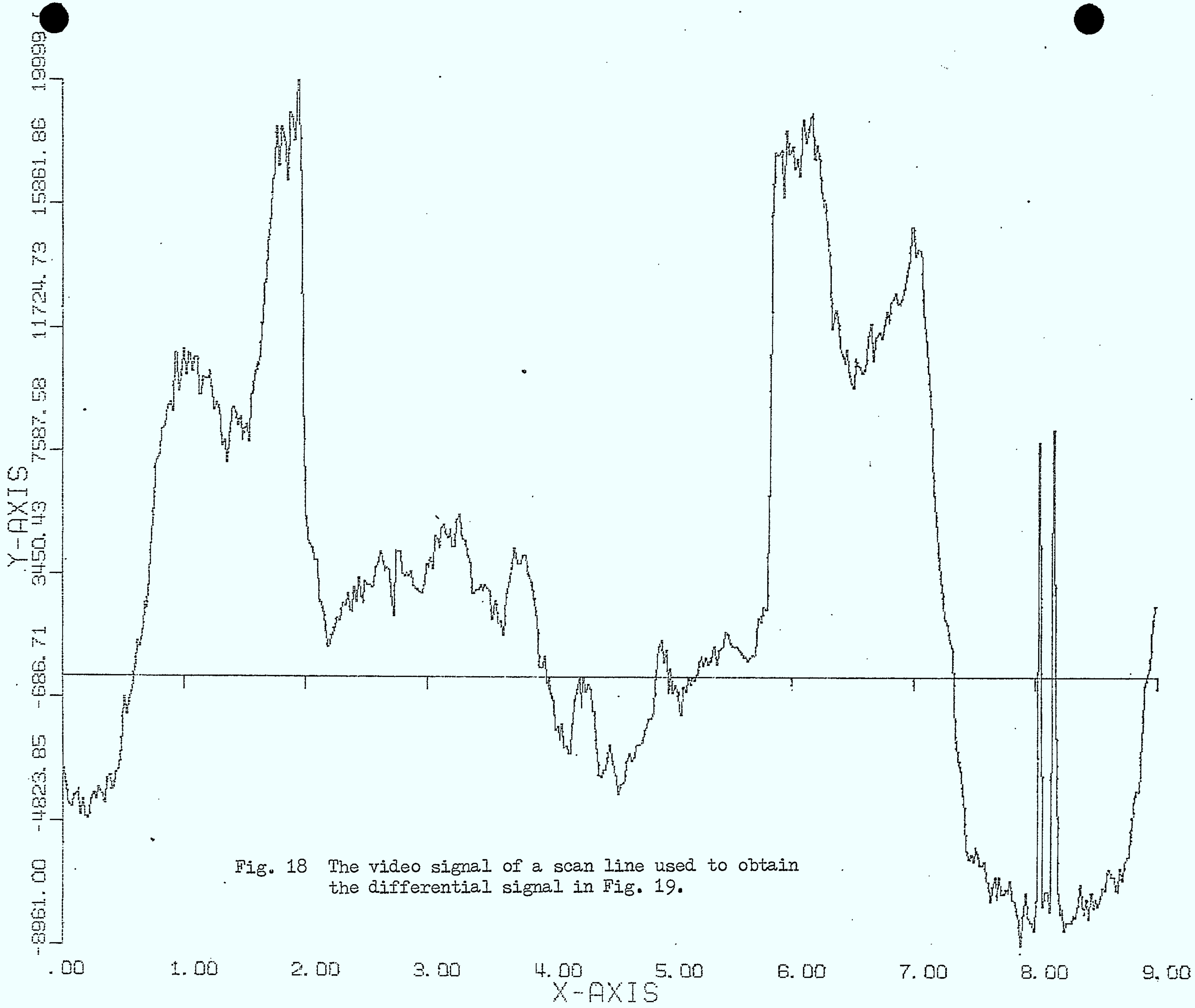

Fig. 18 The video signal of a scan line used to obtain the differential signal in Fig. 19.

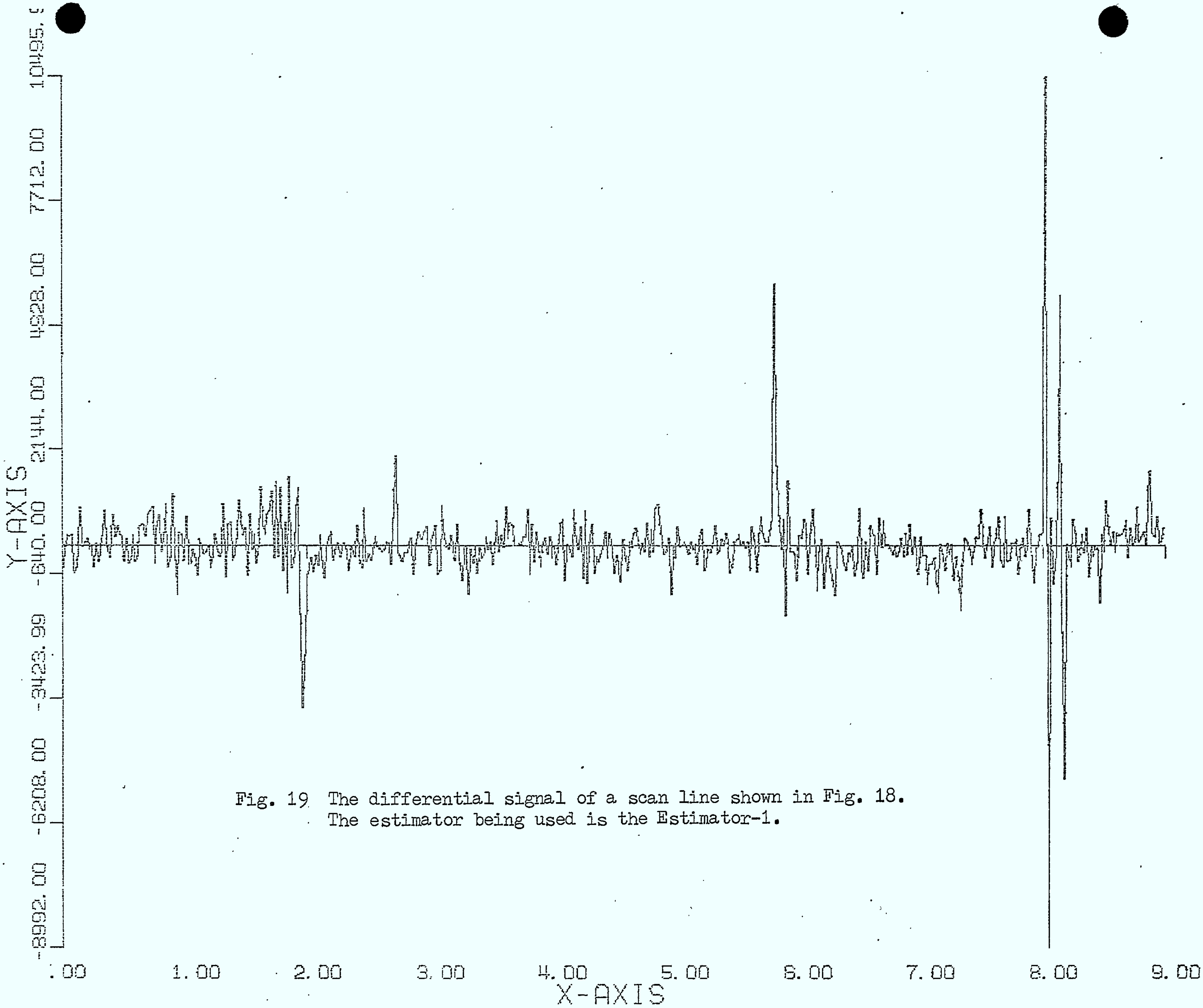

Fig. 19 The differential signal of a scan line shown in Fig. 18.
The estimator being used is the Estimator-1.

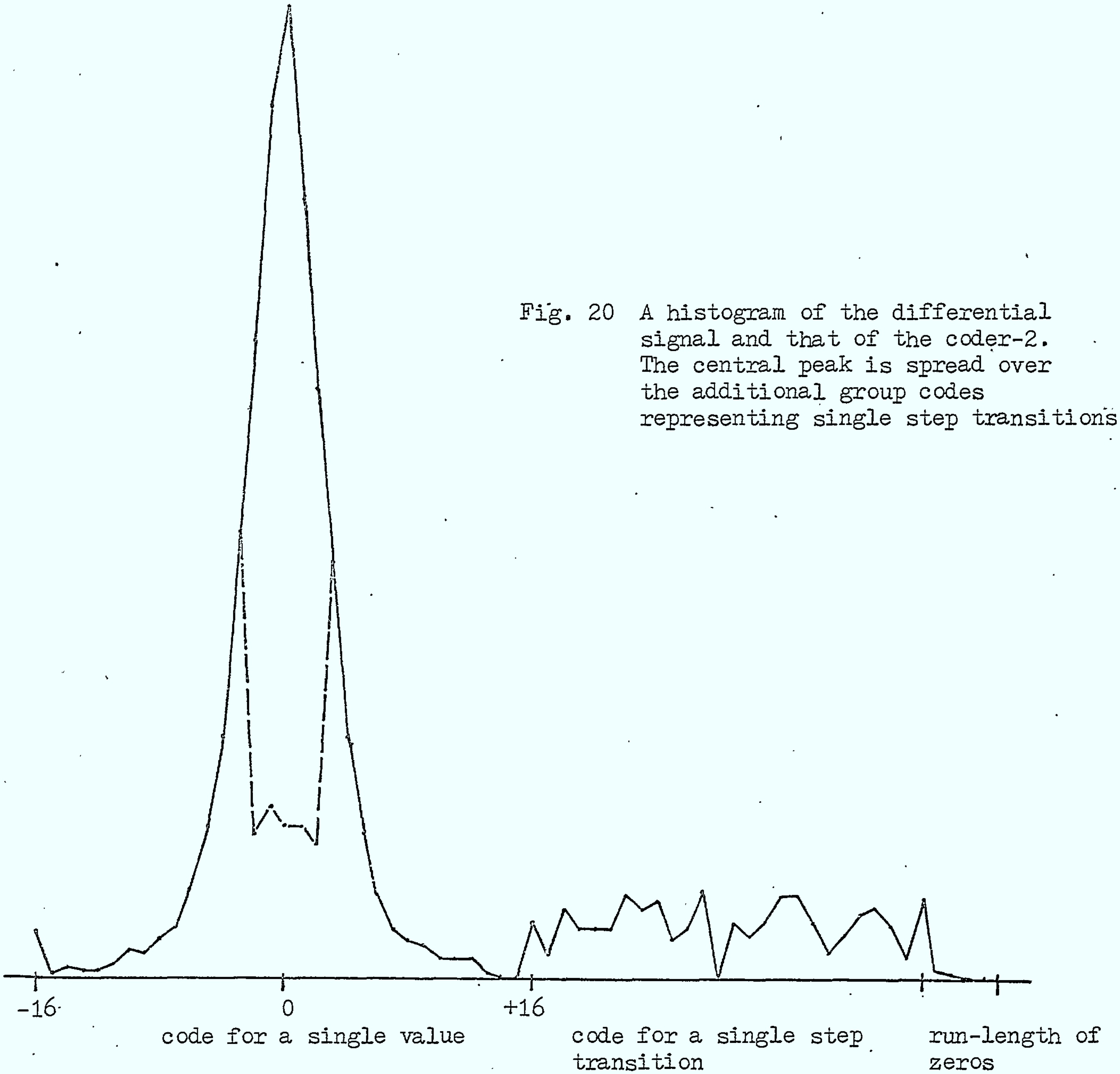

Fig. 20 A histogram of the differential signal and that of the coder-2. The central peak is spread over the additional group codes representing single step transitions.

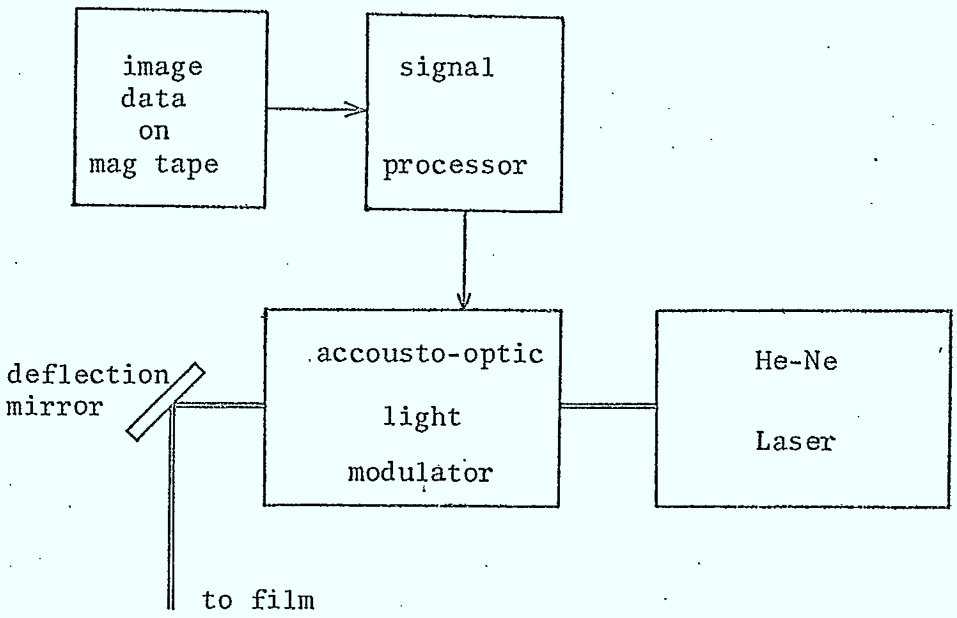

Fig. 21 The laser printer scheme under consideration

TAKAYA, KUNIO

A system for the digital transmission of X-ray pictures over voice grade dial up channels ...

DATE DUE
DATE DE RETOUR
